



*Supplement of*

## **Peatland-VU-NUCOM (PVN 1.0): using dynamic plant functional types to model peatland vegetation, CH<sub>4</sub>, and CO<sub>2</sub> emissions**

Tanya J. R. Lippmann et al.

*Correspondence to:* Tanya J. R. Lippmann ([t.j.r.lippmann@vu.nl](mailto:t.j.r.lippmann@vu.nl))

The copyright of individual parts of the supplement might differ from the article licence.

**Table S1.** Range and scope of current peatland models using PFTs. We've only counted the number of peatland specific PFTs. Some models use more PFTs than what have been counted here.

Model	Gridded	Site specific	PFT competition	CO <sub>2</sub> scheme	CH <sub>4</sub> scheme	Citation
PEATBOG	✓	✓	✓	✓	✓	Wu et al. (2016)
LPJ-WHyMe	✓	-	✓	✓	✓	Wania et al. (2010)
MILLENNIA	-	✓	-	✓	✓	Heinemeyer et al. (2010)
CH4MOD <sub>wetland</sub>	-	✓	-	-	✓	Li et al. (2016)
McGill Wetland Model	-	✓	-	✓	-	Wu et al. (2011)
Holocene Peat Model	-	✓	✓	-	-	Frolking et al. (2010)
CLASS3.6–CTEM	✓	-	-	✓	-	Wu et al. (2016)
ORCHIDEE-PEAT	✓	✓	-	✓	-	Lageron et al. (2018); Krinner et al. (2005); Ringeval et al. (2010)
LPJ-GUESS	✓	✓	✓	✓	-	Smith et al. (2001); Chaudhary et al. (2017)
Bauer	-	✓	-	✓	-	Bauer (2004)
LPJ-WHy	✓	-	✓	-	-	Wania et al. (2009)
GUESS-ROMUL	✓	-	-	✓	-	Yurova et al. (2007)
DYPTOP	✓	✓	-	-	-	Stocker et al. (2014)
LPX-Bern DGVM	✓	-	✓	-	-	Müller and Joos (2020)
Community Land Model	✓	✓	-	-	-	Shi et al. (2015)
CaMP	-	✓	-	✓	✓	Bona et al. (2020)
NUCOM	-	✓	✓	✓	-	Heijmans et al. (2008)
PEATLAND-VU	-	✓	-	✓	✓	van Huissteden et al. (2006)
PVN	-	✓	✓	✓	✓	This publication

## 1 Material and methods

**Table S2.** Soil organic matter (SOM) pools represented by the model, their respective rates of decomposition (k), and their contributing sources.

SOM pool	k [kg C m <sup>-2</sup> year <sup>-1</sup> ]	Source
Microbial biomass	100	Fraction of carbon ( $MI_p$ ) transferred from the decomposition of litter & dead roots, root exudates, peat
Litter and dead roots	50	Above-ground biomass die off and root die off
Root exudates	50	Root exudation as a fraction of root growth (Eq. 19)
Humus	0.05	Fraction of matter ( $HU_p$ ) transferred from the decomposition of litter & dead roots, root exudates, peat
Peat	0.01	Inert carbon from all other SOM pools

**Table S3.** References for parameters in Table 1. VH06 values informed by Peatland-VU van Huissteden et al. (2006, 2009). H16 (HA16) refers to parameters taken directly (adapted) from the NUCOM-BOG model Heijmans et al. (2008). W16 (WA16) refers to values taken directly (adapted) Wu et al. (2016). W09 refers to values taken from Wania et al. (2009). TRY refers to values taken from the TRY database 5.0 ([www.try-db.org](http://www.try-db.org)) Kattge et al. (2020, 2011). W11 (WA11) refers to values taken directly (adapted) Wu et al. (2011). SA03 refers to values informed by Sitch et al. (2003). \*Parameters with available observational data that were previously used either in the calibration of the Peatland-VU model or as model constants.

Parameter	Tall grasses	Sedges	Typha	Sphagnum	Brown moss	Short grass
BS*	HA16	HA16	HA16	H16	H16	HA16
KL	VH06	VH06	VH06	H16	H16	TRY
CBiomassRatio	WA11	WA11	WA11	W11	W11	WA11
RS*	WA16	W16	WA16	H16	H16	HA16
MaxCanopyHeight*	TRY	TRY	TRY	H16	H16	TRY
$T_{MaxPhoto}^*$	WA16	W16	WA16	W16	W16	WA16
$T_{MinPhoto}^*$	WA16	W16	WA16	W16	W16	WA16
$T_{min}^*$	TRY	HA16	HA16	H16	H16	HA16
$T_{minopt}^*$	TRY	TRY	TRY	H16	H16	HA16
$T_{maxopt}^*$	TRY	TRY	TRY	H16	H16	HA16
$T_{max}^*$	TRY	TRY	TRY	H16	H16	HA16
Rc	SA03	SA03	SA03	SA03	SA03	SA03
Rr	SA03	SA03	SA03	SA03	SA03	SA03
Gmax*	HA16	HA16	HA16	H16	H16	HA16
SLA*	HA16	HA16	HA16	H16	H16	TRY
MinLAI*	WA16	W16	WA16	WA16	WA16	WA16
MaxLAI*	WA16	W16	WA16	WA16	WA16	WA16
LEC*	H16	H16	H16	H16	H16	TRY
PIOx*	VH06	VH06	VH06	VH06	VH06	VH06
vP*	VH06	VH06	VH06	VH06	VH06	VH06
MRD*	WA16	W16	WA16	WA16	WA16	WA16
RSX	W09	W09	W09	HA16	HA16	HA16
REX	VH06	VH06	VH06	VH06	VH06	VH06
KSP	VH06	VH06	VH06	VH06	VH06	VH06
LC*	VH06	VH06	VH06	VH06	VH06	VH06
HU	SA03	SA03	SA03	SA03	SA03	SA03
MI	VH06	VH06	VH06	VH06	VH06	VH06
$WL_{min}^*$	TRY	TRY	TRY	H16	H16	HA16
$WL_{minopt}^*$	TRY	TRY	TRY	H16	H16	HA16
$WL_{maxopt}^*$	TRY	TRY	TRY	H16	H16	HA16
$WL_{max}^*$	TRY	TRY	TRY	H16	H16	HA16

## 1.1 Photosynthesis and plant respiration

$$WSF_{t,p} = 1 + LEC_p \cdot LAI_{t,p} - e^{-WG_{t,p}} \quad (1)$$

where,  $WSF$  [-] represents a water stress factor,  $LEC$  [-] represents the Light Extinction Coefficient parameter,  $LAI$  [ $m^2 m^{-2}$ ] represents the leaf area index, and  $WG$  [-] represents the water growth function (Eq. 14).

$$JE_{t,p} = C1_{t,p} \cdot FPAR_{t,p} \cdot PAR_t \quad (2)$$

where,  $JE$  [ $\text{kg C m}^{-2} \text{ day}^{-1}$ ] describes the response of photosynthesis to photosynthetically active radiation (PAR),  $C1$  [ $\text{kg mol}^{-1}$ ] is defined by Eq. 3 (Haxeltine and Prentice, 1996),  $FPAR$  [-] is the fraction of incoming PAR absorbed by vegetation (Eq. 7),  $PAR$  [ $\text{mol m}^{-2} \text{ day}^{-1}$ ] represents PAR.

$$C1_{t,p} = \frac{pi - \Gamma}{pi + \Gamma} \cdot Cmass \cdot \phi_{T,t,p} \cdot \alpha_a \cdot \alpha \quad (3)$$

where,  $\alpha$  [-] has value 0.08, the intrinsic quantum efficiency for  $\text{CO}_2$  uptake.  $\alpha_a$  [-] is a scaling constant with value 0.5.  $Cmass$  [ $\text{kg mol}^{-1}$ ] has value 0.012, the molar mass of carbon.  $pi$  [Pa] refers to the intercellular  $\text{CO}_2$  partial pressure,  $\Gamma$  [Pa] is the  $\text{CO}_2$  compensation point calculated by Eq. S16 (Haxeltine and Prentice, 1996).  $\phi_{T,t,p}$  [-] is calculated using Eq. 4 where, PFT specific parameters were applied to the temperature stress function of the Peatland-VU model (Mi et al., 2014):

$$\phi_{T,t,p} = TFL_{t,p} \cdot TFH_{t,p} \quad (4)$$

where,  $TFL$  [-] and  $TFH$  [-] represent temperature stress factors for low and high temperatures, respectively:

$$TFL_{t,p} = \frac{1}{1 + e^{T1_p \cdot (T2_p - T_t)}}, \quad (5)$$

$$TFH_{t,p} = 1 - 0.01 \cdot e^{T3_p \cdot (T_t - T_{max,p})} \quad (6)$$

where,  $T1$  [ $^\circ\text{C}^{-1}$ ],  $T2$  [ $^\circ\text{C}^{-1}$ ],  $T3$  [ $^\circ\text{C}^{-1}$ ] are PFT constants:

$$T1_p = \frac{2 \cdot \ln(1/0.99 - 1)}{T_{MinPhoto,p} - T_{min,p}}, \quad (7)$$

$$T2_p = \frac{\ln(0.99/0.01)}{2 \cdot T_{MinPhoto,p} + T_{maxopt,p}}, \quad (8)$$

$$T3_p = \frac{\ln(0.99/0.01)}{T_{MaxPhoto,p} - T_{maxopt,p}} \quad (9)$$

where,  $T_{MinPhoto}$ ,  $T_{min}$ ,  $T_{maxopt}$ ,  $T_{MaxPhoto}$  are PFT parameters (Table 1).  $JC$  [ $\text{kg C m}^{-2} \text{ day}^{-1}$ ] describes the Rubisco limited rate of photosynthesis (Haxeltine and Prentice, 1996):

$$JC_{t,p} = C2 \cdot VM_{t,p} \quad (10)$$

where,  $C2$  [-] is calculated using Eq. S14. The maximum daily rate of net photosynthesis is represented by  $VM$  [ $\text{kg C m}^{-2} \text{ day}^{-1}$ ], calculated using Eq. S11 (Haxeltine and Prentice, 1996).

$$VM_{t,p} = \frac{FPAR_{t,p} \cdot PAR_t}{Rr_p} \cdot \frac{C1}{C2} \cdot (s_{t,p} \cdot (2 \cdot \theta - 1) - \sigma_{t,p} \cdot (2 \cdot s_{t,p} \cdot \theta - C2)) \quad (11)$$

where,  $Rr$  is the leaf respiration coefficient [-],  $\sigma$  [-] is calculated using Eq. S12,  $s$  [ $\text{kg C m}^{-2}$ ] is calculated with Eq. 13,  $\theta$  [-] is a co-limitation constant that has value 0.7 (Haxeltine and Prentice, 1996).

$$\sigma_{t,p} = \sqrt{1 - \frac{C2 - s_{t,p}}{C2 - \theta \cdot s_{t,p}}} \quad (12)$$

$$s_{t,p} = \frac{Rr_p}{DL_t} \quad (13)$$

where,  $DL$  [day $^{-1}$ ] is the day length (Haxeltine and Prentice, 1996).

$$35 \quad C2 = \frac{pi - \gamma}{pi + KC \cdot KCC} \quad (14)$$

where,  $\gamma$  [-] is a constant with value, 0.7.  $O_2$  [Pa] is the partial pressure of oxygen (Haxeltine and Prentice, 1996),  $KC$  [Pa] is the Michaelis constant for  $CO_2$  with a value of 30, and  $KCC$  [-] is calculated using Eq. S15 (Haxeltine and Prentice, 1996).

$$KCC = \frac{O_2}{K0} + 1 \quad (15)$$

,  $K0$  [Pa] is the Michaelis constant for  $O_2$  and has value 0.03,  $O_2$  [Pa] represents the partial pressure of oxygen and has value 20,900 (Haxeltine and Prentice, 1996).

$$\Gamma = \frac{O_2}{2 \cdot \tau} \quad (16)$$

where,  $\tau$  [-] is the  $CO_2$  to  $O_2$  specificity ratio and has value 2,600 (Haxeltine and Prentice, 1996).

$$pi = \Gamma \cdot pa \quad (17)$$

where,  $pa$  [Pa] is the ambient partial pressure of  $CO_2$  and  $\gamma$  is a unitless constant, 0.7 (Haxeltine and Prentice, 1996).

## 45 1.2 Below-ground SOM decomposition

The decomposition rate of each SOM is impacted by environmental conditions:

$$ke_S = k_S \cdot f_{ae} \cdot f_m \cdot f_T \cdot f_{pH} \cdot f_{prim} \quad (18)$$

where,  $k$  [kg C m $^{-2}$  day $^{-1}$ ], the decomposition rates of each SOM reservoir are defined in Table: S2.  $f_{ae}$  represents a correction factor for soil aeration,  $f_m$  represents a correction factor for soil moisture,  $f_T$  represents the correction factor for soil temperature,  $f_{pH}$  represents a correction factor for soil pH,  $f_{prim}$  represents the correction factor for priming effects (van Huissteden et al., 2006).

## 1.3 Methane processes

The concentration of each layer (Eq. 19) is dependent on plant transported  $CH_4$  ( $Qpl$ ) and the below-ground processes: anaerobic  $CH_4$  production ( $Rpr$ ),  $CH_4$  oxidation ( $Rox$ ), ebullition ( $Qeb$ ), and diffusion of  $CH_4$  through soil ( $Fdiff$ ). After the calculation of  $CH_4$  concentration of each soil layer before, the transport mechanisms are summed to obtain the  $CH_4$  flux at the surface (Eq. 19). The equations for  $CH_4$  diffusion (Eq. S21), oxidation (Eq. S27), production (Eq. S26), and ebullition (Eq. S24) are elaborately described in Walter and Heimann (2000a) and van Huissteden et al. (2006).

$$60 \quad \frac{\delta}{\delta t} C_{CH_4,t,z} = Rpr_{t,z} - \sum_{p=1}^P (Qpl_{t,p,z}) - \frac{\delta}{\delta z} Fdiff_{t,z} - Qeb_{t,z} - Rox_{t,z} \quad (19)$$

where,  $C_{CH_4}$  represents the  $CH_4$  concentration [ $\mu M m^{-3}$ ].  $Rpr$  [ $\mu M m^{-3}$  day $^{-1}$ ] is the temperature dependent production of  $CH_4$  (Eq. S26), where warmer temperatures lead to enhanced  $CH_4$  production rates (Walter and Heimann, 2000a).  $Qpl$  [ $\mu M m^{-3}$  day $^{-1}$ ] is the  $CH_4$  flux by plant roots Eq. 30.  $Qeb$  [ $\mu M m^{-3}$  day $^{-1}$ ] represents ebullition of  $CH_4$  (Eq. S24).  $Rox$  [ $\mu M m^{-3}$  day $^{-1}$ ] is the temperature dependent removal of  $CH_4$  by methanotrophic oxidation of  $CH_4$  to  $CO_2$  in the soil (Eq. S27) (Walter and Heimann, 2000a). The diffusive flux,  $Fdiff_{t,z}$  is calculated using Fick's first law (Sect. 1.3.1).

### 1.3.1 Methane diffusion

65 The diffusive flux,  $F_{diff,t,z}$  [ $\mu\text{M m}^{-2} \text{ day}^{-1}$ ] is calculated using Fick's first law (Walter and Heimann, 2000a):

$$F_{diff,t,z} = -D_{CH_4,z} \cdot \frac{\delta}{\delta z} C_{CH_4,t,z} \quad (20)$$

where,  $D$  [-] is the diffusion coefficient of  $\text{CH}_4$  with depth, calculated using the Penman relation using a tortuosity coefficient (0.66):

$$D_{CH_4,z} = D_i \cdot 0.66 \cdot f_{coarse} \quad (21)$$

70 where,  $D_i$  has the value  $1.728 \text{ m}^{-2} \text{ day}^{-1}$  in unsaturated layers, and  $10^{-4} 1.728 \text{ m}^{-2} \text{ day}^{-1}$  in saturated layers (Walter and Heimann, 2000a),  $f_{coarse}$  [-] denotes the relative volume of large pores, where diffusion is assumed to be possible (Walter and Heimann, 2000a). Methane concentration estimates represent the concentration at the middle of the soil layer, whereas the diffusion coefficients are calculated at the layer boundaries using the lower boundary condition:

$$\frac{\delta}{\delta z} C_{CH_4,t,z=nsoil} = 0 \quad (22)$$

75 and the upper boundary condition:

$$\frac{\delta}{\delta z} C_{CH_4,t,z=u+0.04m} = C_{atm} \quad (23)$$

where,  $u$  is either the  $WL$  or the soil surface,  $C_{atm}$  is the atmospheric  $\text{CH}_4$  concentration of  $0.076 \mu\text{M}$  (Walter and Heimann, 2000a).

### 1.3.2 Methane ebullition

80  $Q_{eb,t,z} = -k_m \cdot f(C_{CH_4}) \cdot (C_{CH_4,t,z} - MethaneMaxConc)$  (24)

where,  $K_m$  [ $\text{day}^{-1}$ ] is constant of value,  $1/24$ .  $f(C_{CH_4})$  is a step function with the value 1, if the  $\text{CH}_4$  concentration ( $C_{CH_4}$ ) is greater than  $C_{thresh}$ , and has the value 0 otherwise. If the concentration of  $\text{CH}_4$  exceeds  $MethaneMaxConc$  (Table S4), ebullition occurs (Walter and Heimann, 2000a). In the layers above the water level,  $Q_{eb}$  has value 0. The ebullitive  $\text{CH}_4$  flux ( $Feb$ ) is obtained by integrating  $Q_{eb}$  over the saturated zone:

$$85 Feb_t = \int_{z=nsoil}^{WL_t} Q_{eb,t,z} dz \quad (25)$$

where,  $Feb$  [ $\mu\text{M m}^{-2} \text{ day}^{-1}$ ] represents the ebullitive flux,  $nsoil$  [m] is the lower boundary of the soil column. If the water level is at the surface or above the soil surface,  $Feb$  contributes directly to Eq. 29, the  $\text{CH}_4$  flux into the atmosphere. If the water level is below the soil surface, the amount of  $\text{CH}_4$  reaching the lowest unsaturated soil layer in the form of ebullition is added to the  $\text{CH}_4$  concentration of that layer.

### 90 1.3.3 Methane production

$$Rpr_{t,z} = MethaneR0 \cdot f_{org}(z) \cdot f_{in}(t) \cdot f(T) \cdot MethaneQ10^{\frac{T_{t,z} - T_{mean}}{10}} \quad (26)$$

where,  $MethaneR0$  [ $\text{kg M day}^{-1}$ ] is a constant rate factor where  $1\text{M} = 1 \text{ mol L}^{-1}$ ,  $f_{org}(z)$  is the fraction of substrate available of [-],  $f(T)$  is 1 if  $T_t > 0$ ,  $T_{mean}$  refers to the annual mean soil temperature [deg C],  $MethaneQ10$  [-, Table S4] refers to the extent that  $\text{CH}_4$  production is dependent on soil temperature.



**Figure S1.** Examples of the vegetation and the chambers at the Horstermeer (left) and the Ilperveld (right) sites.

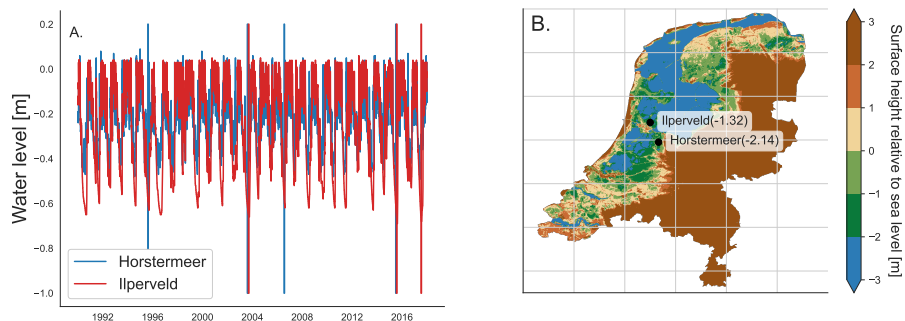


**Figure S2.** A. The water table heights relative to the land surface over the simulated period, 1990-2018. The sign convention in this paper is that the water table depth is assigned as a negative value when the water table is below the surface. B. The location of the 2 field sites and the land surface height in the Netherlands.

#### 95 1.3.4 Methane oxidation

$$Rox_{t,z} = \frac{\text{MethaneVmax} \cdot C_{CH_4}(t,z)}{\text{MethaneKm} + C_{CH_4}} \cdot \text{MethaneOxQ10}^{\frac{T_{t,z} - T_{mean}}{10}} \quad (27)$$

where, MethaneVmax [ $\mu\text{mol day}^{-1}$ ], MethaneKm [ $\mu\text{mol}$ ], MethaneOxQ10 [-] are constants defined in (Table S4).  $C_{CH_4}$  denotes the  $\text{CH}_4$  concentration.

#### 1.4 Two peatland sites

#### 100 1.5 Model Calibration

The KGE performance metric evaluates the temporal dynamics, bias, and variability on a scale from -infinity to 1, with 1 being a perfect simulation Eq. 28.

$$KGE = 1 - \sqrt{(r - 1)^2 + (\alpha - 1)^2 + (\beta - 1)^2} \quad (28)$$

$$\alpha = \sigma_s / \sigma_o \quad (29)$$

$$\beta = \mu_s / \mu_o \quad (30)$$

**Table S4.** Model input parameters used in this study. \*These variables were used in the calibration of the Horstermeer and Ilperveld site simulations.

Parameter	Units	Description
AnaerobeLagFactor*	days	The time lag for development of sufficiently anaerobic conditions for methanogenesis after rapid saturation of a layer by rapid water table rise.
EndDate	DD/MM/YYYY	End date of model simulation
GrowFuncConst*	-	Proportionality constant for use of different production models for plant transport in methane model
GwFile	m	Filename of file with daily water table data
HalfSatPoint*	-	Correction factor of the aerobic decomposition for poor aeration of the soil by high water saturation
Harvest	-	First number is day of the year. Second number is harvest height.
InitMethane	mmol m <sup>-3</sup>	Initial methane concentration in each soil layer
MethaneERateC*	day <sup>-1</sup>	Ebullition rate constant
MethaneKm	μmol	Km is a Michaelis-Menten coefficient used to calculate CH <sub>4</sub> oxidation (Walter and Heimann, 2000b)
MethaneMaxConc*	μmol m <sup>-3</sup>	Maximum methane concentration in pore water. Above this value, ebullition occurs
MethaneOxQ10*	-	Constant used to relate CH <sub>4</sub> oxidation and soil temperature (Walter and Heimann, 2000b)
MethaneQ10*	-	Constant used to relate CH <sub>4</sub> production and soil temperature (Walter and Heimann, 2000b)
MethaneR0*	mmol day <sup>-1</sup> m <sup>-3</sup>	Methane production rate factor for fresh organic carbon
MethaneR0Pt*	mmol day <sup>-1</sup> m <sup>-3</sup>	Methane production rate factor for old peat
MethaneReservoirs	-	This parameter specifies which reservoirs are being used (1.0) for calculation of CH <sub>4</sub> production
MethaneVmax*	μmol day <sup>-1</sup>	Vmax is a Michaelis-Menten coefficient used to calculate CH <sub>4</sub> oxidation (Walter and Heimann, 2000b)
MolAct*	-	Aerobic organic matter decomposition constant
PARFile	J cm <sup>-2</sup> day <sup>-1</sup>	Filename of file with daily radiation data
PFTFiles	-	Filenames
PartialAnaerobe*	-	Constant used to calculate CH <sub>4</sub> production in anaerobic microsites above the water table
PrimProdC	-	Constant used to estimate anaerobic CO <sub>2</sub> production
SatCorr	-	Constant for CH <sub>4</sub> production in saturated topsoil
StartDate	DD/MM/YYYY	Start date of model simulation
TFile	°C	Filename of file with daily temperature data
KT	°C	Reference temperature
ThermDiff	m <sup>2</sup> day <sup>-1</sup>	Thermal diffusivity
VegTScalingFactor*	-	Constant for calculating air to soil surface temperature gradient

where  $r$  is the Pearson correlation coefficient between model simulations and observations,  $\alpha$  is a measure of relative variability (ratio between the STD of simulated and observed fluxes),  $\beta$  represents the bias (ratio between the mean of simulated and observed fluxes).  $\mu_s$  and  $\mu_o$  are the mean of simulated and observed fluxes and  $\sigma_s$  and  $\sigma_o$  are the STD of simulated and observed fluxes.

**Table S5.** Model input parameters to create the soil profile.

Parameter	Units	Description
CNRatio	-	C:N ratio for each soil horizon
DBD	$\text{kg m}^{-3}$	Dry bulk density of each soil horizon
Horizons	-	Depth of soil horizons
InitResn	-	Initial fraction of OM found in each SOM reservoir in the nth soil horizon
LayerpFn	$\text{m}^3 \text{ m}^{-3}$	pF curve for the nth soil horizon
LayerpH	pH	pH for each horizon
NrHorizons	-	Number of soil horizons
PercOrg	%	Percentage of total dry weight that is OM for each horizon
SandFraction	-	Fraction of each soil horizon that is sand
pFVal	$\log \text{ cm H}_2\text{O}$	Soil moisture potential for each soil horizon

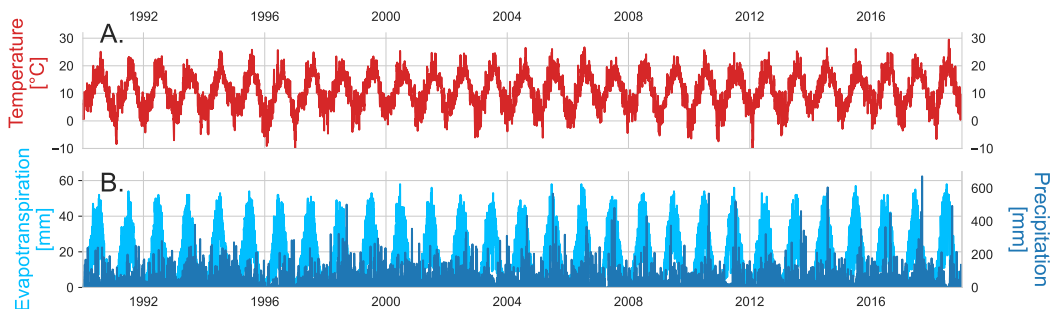


**Figure S3.** Daily precipitation, evapotranspiration, and temperature observations recorded at nearby weather station, Schiphol. Shown for the years 1990 - 2019.

**Table S6.** Model input parameters for the Horstermeer site simulations.

Parameter	Value
AnaerobeLagFactor	0.0935
EndDate	31/12/2017
GrowFuncConst	4.0
GwFile	HorstermeerGW.txt
HalfSatPoint	0.1
Harvest	-
InitMethane	500, 500, 1000, 1000, 1000, 1000, 1000, 1000, 1000, 1000, 1000, 1000, 1000, 1000
MethaneERateC	0.5
MethaneKm	5.0
MethaneMaxConc	20000
MethaneOxQ10	1.60
MethaneQ10	16
MethaneR0	5.51
MethaneR0Pt	0.000926
MethaneReservoirs	0, 1, 1, 1, 1, 1, 0
MethaneVmax	5.0
MolAct	201286
PARFile	SchipholRad.txt
PFTFiles	Typha.txt, TallGrasses.txt, Sedges.txt, BrownMoss.txt
PartialAnaerobe	1.11
PrimProdC	0.9
SatCorr	0.0
StartDate	01/01/1990
TFile	SchipholTemp.txt
KT	10
ThermDiff	-1.0
VegTScalingFactor	1.0

**Table S7.** Model input parameters for the Ilperveld site simulations.

Parameter	Value
AnaerobeLagFactor	0.0364
EndDate	31/12/2017
GrowFuncConst	1
GwFile	ILPGW.txt
HalfSatPoint	0.8
Harvest	186 0.15; 268 0.15
InitMethane	100, 100, 500, 1000, 1000, 2000, 3000, 8000, 8000, 10000, 10000, 10000, 10000, 10000
MaxProd	0.005
MethaneERateC	0.3
MethaneKm	5.0
MethaneMaxConc	30477
MethaneOxQ10	2.0
MethaneQ10	8.05
MethaneR0	1.44
MethaneR0Pt	0.00109
MethaneReservoirs	0, 1, 1, 1, 1, 0, 0
MethaneVmax	15.43
MolAct	22500
PARFile	SchipholRad.txt
PFTFiles	ShortGrass.txt, SphagnumMoss.txt, BrownMoss.txt, TallGrasses.txt
PartialAnaerobe	5.56
PrimProdC	1.0
SatCorr	0.0
StartDate	01/01/1990
TFile	SchipholTemp.txt
KT	9.43
ThermDiff	-1.0
VegTScalingFactor	0.6

**Table S8.** Input parameters to create the soil profile for the Horstermeer site simulations.

Parameter	Value
CNRatio	13.17, 13.75, 14.88, 15.83, 17.02, 25.04
DBD	346.42, 461.00, 465.25, 482.00, 371.00, 330.50
Horizons	0.1, 0.2, 0.3, 0.4, 0.5, 1.5
InitRes1	0.69, 0.0, 0.0, 0.0, 0.01, 0.0, 0.3
InitRes2	0.92, 0.0, 0.0, 0.0, 0.0, 0.0, 0.08
InitRes3	0.93, 0.0, 0.0, 0.0, 0.0, 0.0, 0.07
InitRes4	0.93, 0.0, 0.0, 0.0, 0.0, 0.0, 0.07
InitRes5	0.93, 0.0, 0.0, 0.0, 0.0, 0.0, 0.07
InitRes6	0.93, 0.0, 0.0, 0.0, 0.0, 0.0, 0.07
LayerpF1	0.834, 0.826, 0.812, 0.769, 0.686, 0.637, 0.320
LayerpF2	0.785, 0.772, 0.760, 0.747, 0.703, 0.674, 0.320
LayerpF3	0.772, 0.766, 0.757, 0.744, 0.729, 0.714, 0.320
LayerpF4	0.778, 0.778, 0.777, 0.766, 0.754, 0.733, 0.320
LayerpF5	0.835, 0.831, 0.830, 0.830, 0.797, 0.770, 0.320
LayerpF6	0.835, 0.831, 0.830, 0.830, 0.797, 0.770, 0.320
LayerpH	5.6, 5.8, 5.82, 5.35, 5.50, 5.93
NrHorizons	6
PercOrg	41.36, 37.46, 45.09, 35.26, 29.66, 47.91
SandFraction	0.05, 0.0, 0.0, 0.0, 0.0, 0.0
pFVal	0.0, 0.4, 1.0, 1.5, 1.8, 2.0, 4.2

**Table S9.** Input parameters to create the soil profile for the Ilperveld site simulations.

Parameter	Value
CNRatio	13.17, 13.75, 14.88, 15.83, 17.02, 25.04
DBD	430.1, 227.2, 73.6, 102.5, 90.0, 104.35
Horizons	0.1, 0.2, 0.3, 0.4, 0.5, 1.5
InitRes1	0.69, 0.0, 0.0, 0.0, 0.01, 0.0, 0.3
InitRes2	0.92, 0.0, 0.0, 0.0, 0.0, 0.0, 0.08
InitRes3	0.93, 0.0, 0.0, 0.0, 0.0, 0.0, 0.07
InitRes4	0.93, 0.0, 0.0, 0.0, 0.0, 0.0, 0.07
InitRes5	0.93, 0.0, 0.0, 0.0, 0.0, 0.0, 0.07
InitRes6	0.93, 0.0, 0.0, 0.0, 0.0, 0.0, 0.07
LayerpF1	0.995, 0.986, 0.971, 0.946, 0.686, 0.637, 0.320
LayerpF2	0.986, 0.947, 0.890, 0.864, 0.703, 0.674, 0.320
LayerpF3	0.975, 0.950, 0.896, 0.864, 0.729, 0.714, 0.320
LayerpF4	0.986, 0.955, 0.894, 0.856, 0.754, 0.733, 0.320
LayerpF5	0.987, 0.964, 0.899, 0.863, 0.797, 0.770, 0.320
LayerpF6	0.981, 0.973, 0.916, 0.884, 0.797, 0.770, 0.320
LayerpH	5.6, 5.8, 5.82, 5.35, 5.50, 5.93
NrHorizons	6
PercOrg	41.36, 37.46, 45.09, 35.26, 29.66, 47.91
SandFraction	0.05, 0.0, 0.0, 0.0, 0.0, 0.0
pFVal	0.0, 0.4, 1.0, 1.5, 1.8, 2.0, 4.2

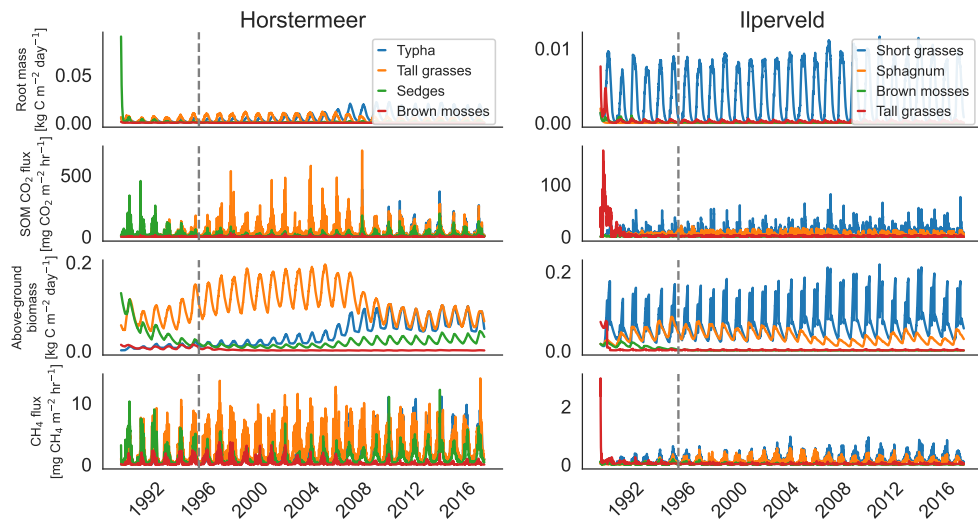


**Figure S4.** The model spin-up (i.e. model stabilisation) period for the Ilperveld and Horstermeer site simulations, beginning in the year 1990, for the root mass, above-ground biomass, SOM  $\text{CO}_2$  flux, and  $\text{CH}_4$  flux of each PFT. The spin-up period was determined by the amount of model time needed for these pools to cease fluctuating following model initialisation.

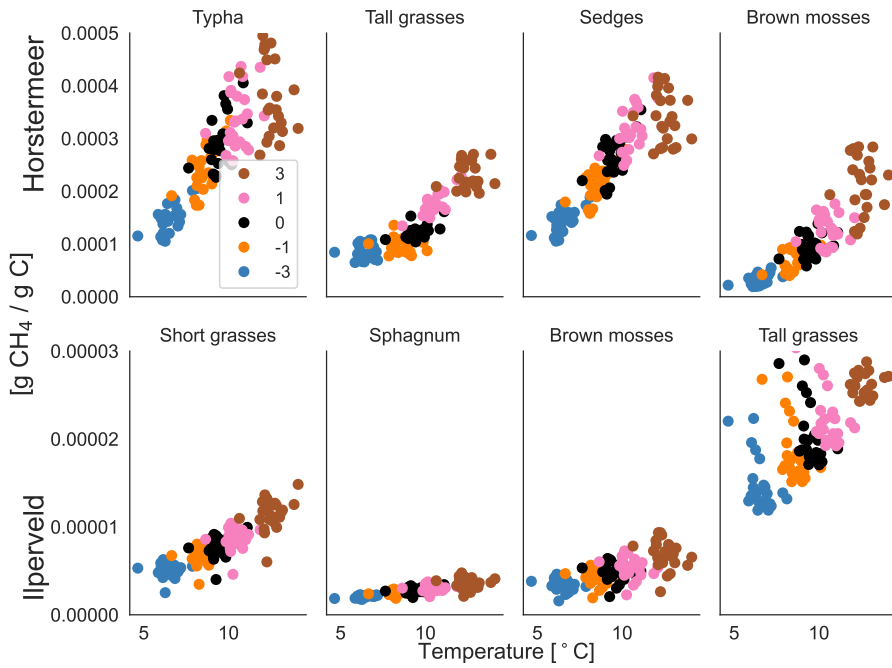


**Figure S5.** The results of the sensitivity tests show the relationship between different temperature inputs and the mean daily plant transported  $\text{CH}_4$  for each year (shown as a fraction of the mean daily litter & root mass for each year), for each of the PFTs at the Horstermeer site (top row) and Ilperveld site (bottom row). Temperature input was increased and decreased by 1 & 3  $^{\circ}\text{C}$ , respectively. The legend shows the input change in  $^{\circ}\text{C}$  where,  $\pm$  signs in front of the legend labels show the direction of change. Note the different y axes between the top and bottom panels.

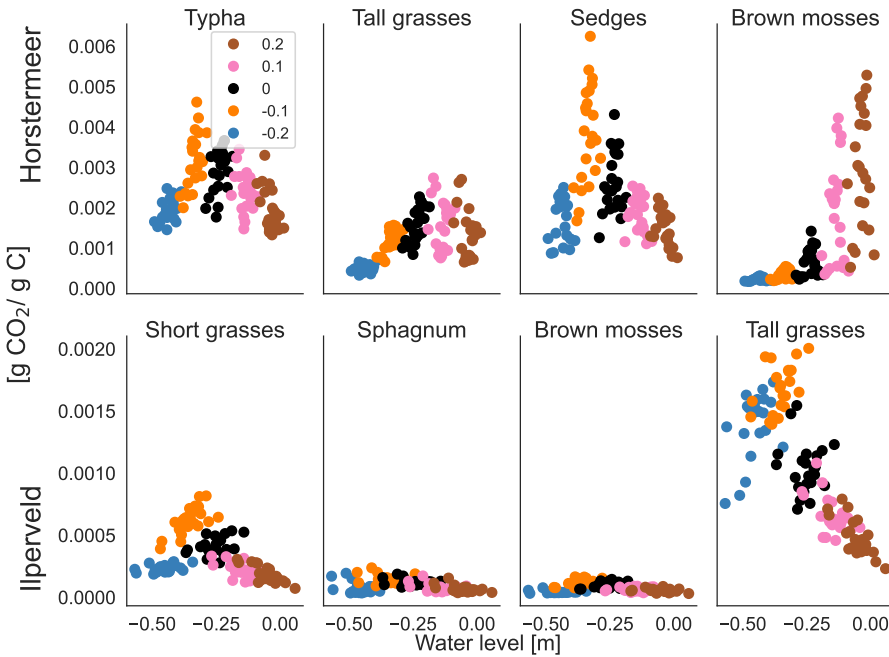


**Figure S6.** The results of the sensitivity tests show the relationship between different water level inputs and the mean daily below-ground CO<sub>2</sub> flux for each year (shown here as a fraction of the mean daily litter & root mass for each year), for each of the PFTs at the Horstermeer site (top row) and Ilperveld site (bottom row). Water level input was decreased by 0.1 & 0.2 m and increased by 0.1 & 0.2 m, respectively. The legend shows the input change, where ± signs in front of the legend labels indicate the direction of change. Note the different y axes between the top and bottom panels.

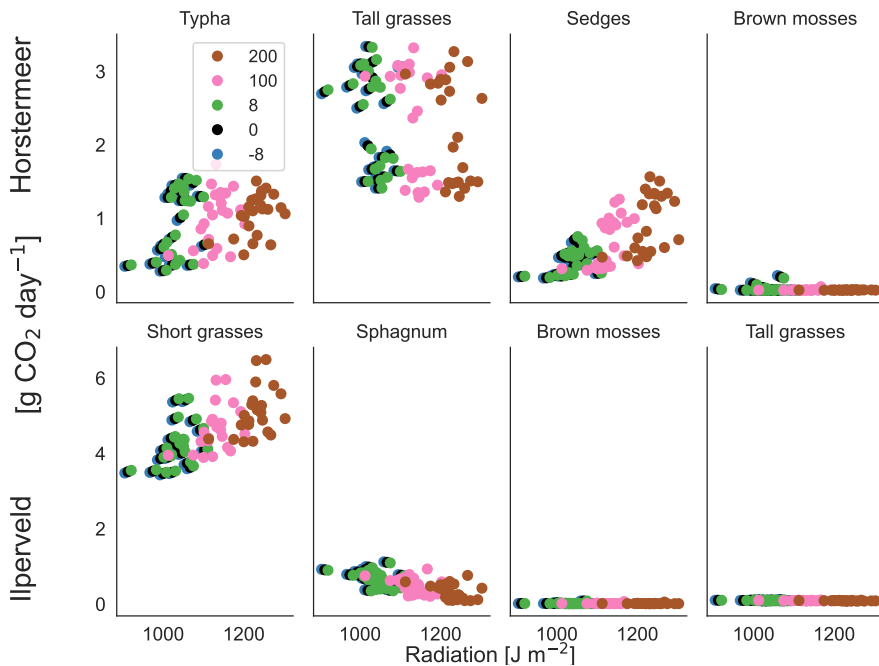


**Figure S7.** The results of the sensitivity tests show the relationship between the different radiation inputs and the mean daily GPP for each year, for each of the PFTs at the Horstermeer site (top row) and Ilperveld site (bottom row). Radiation input was increased by 8, 100 and 200  $\text{J m}^{-2}$ , and decreased by 8  $\text{J m}^{-2}$ . The legend shows the input change in  $\text{J m}^{-2}$  where, ± signs in front of the legend labels show the direction of change.

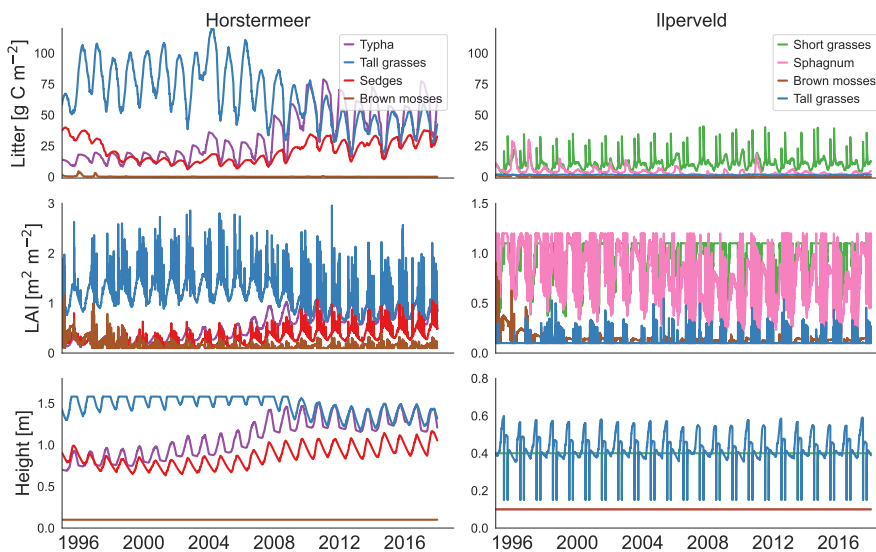


**Figure S8.** Vegetation dynamics. The results of the Horstermeer site simulation are represented in the left column and the results of the Ilperveld site simulation are represented in the right column.

110 **References**

- Bauer, I. E.: Modelling effects of litter quality and environment on peat accumulation over different time-scales, *Journal of Ecology*, 92, 661–674, <https://doi.org/10.1111/j.0022-0477.2004.00905.x>, 2004.
- Bona, K. A., Shaw, C., Thompson, D. K., Hararuk, O., Webster, K., Zhang, G., Voicu, M., and Kurz, W. A.: The Canadian model for peatlands (CaMP): A peatland carbon model for national greenhouse gas reporting, *Ecological Modelling*, 431, 109–164, <https://doi.org/10.1016/j.ecolmodel.2020.109164>, 2020.
- Chaudhary, N., Miller, P. A., and Smith, B.: Modelling Holocene peatland dynamics with an individual-based dynamic vegetation model, *Biogeosciences*, 14, 2571–2596, <https://doi.org/10.5194/bg-14-2571-2017>, 2017.
- Frolking, S., Roulet, N. T., Tuittila, E., Bubier, J. L., Quillet, A., Talbot, J., and Richard, P. J. H.: A new model of Holocene peatland net primary production, decomposition, water balance, and peat accumulation, *Earth System Dynamics*, 1, 1–21, <https://doi.org/10.5194/esd-1-1-2010>, <https://esd.copernicus.org/preprints/1/115/2010/>, <https://esd.copernicus.org/articles/1/1/2010/>, 2010.
- Haxeltine, A. and Prentice, I. C.: BIOME3: An equilibrium terrestrial biosphere model based on ecophysiological constraints, resource availability, and competition among plant functional types, *Global Biogeochemical Cycles*, 10, 693–709, <https://doi.org/10.1029/96GB02344>, <http://doi.wiley.com/10.1029/96GB02344>, 1996.
- Heijmans, M. M., Mauquoy, D., Van Geel, B., and Berendse, F.: Long-term effects of climate change on vegetation and carbon dynamics in peat bogs, *Journal of Vegetation Science*, 19, 307–320, <https://doi.org/10.3170/2008-8-18368>, <https://www.scopus.com/inward/record.url?eid=2-s2.0-41849115693&partnerID=40&md5=650f510b7f8fb783728dc3e00073b873>, 2008.
- Heinemeyer, A., Croft, S., Garnett, M. H., Gloor, E., Holden, J., Lomas, M. R., and Ineson, P.: The MILLENNIA peat cohort model: Predicting past, present and future soil carbon budgets and fluxes under changing climates in peatlands, *Climate Research*, 45, 207–226, <https://doi.org/10.3354/cr00928>, 2010.
- Kattge, J., Díaz, S., Lavorel, S., Prentice, I. C., Leadley, P., Bönisch, G., Garnier, E., Westoby, M., Reich, P. B., Wright, I. J., Cornelissen, J. H., Violle, C., Harrison, S. P., Van Bodegom, P. M., Reichstein, M., Enquist, B. J., Soudzilovskaia, N. A., Ackerly, D. D., Anand, M., Atkin, O., Bahn, M., Baker, T. R., Baldocchi, D., Bekker, R., Blanco, C. C., Blonder, B., Bond, W. J., Bradstock, R., Bunker, D. E., Casanoves, F., Cavender-Bares, J., Chambers, J. Q., Chapin, F. S., Chave, J., Coomes, D., Cornwell, W. K., Craine, J. M., Dobrin, B. H., Duarte, L., Durka, W., Elser, J., Esser, G., Estiarte, M., Fagan, W. F., Fang, J., Fernández-Méndez, F., Fidelis, A., Finegan, B., Flores, O., Ford, H., Frank, D., Freschet, G. T., Fyllas, N. M., Gallagher, R. V., Green, W. A., Gutierrez, A. G., Hickler, T., Higgins, S. I., Hodgson, J. G., Jalili, A., Jansen, S., Joly, C. A., Kerkhoff, A. J., Kirkup, D., Kitajima, K., Kleyer, M., Klotz, S., Knops, J. M., Kramer, K., Kühn, I., Kurokawa, H., Laughlin, D., Lee, T. D., Leishman, M., Lens, F., Lenz, T., Lewis, S. L., Lloyd, J., Llusià, J., Louault, F., Ma, S., Mahecha, M. D., Manning, P., Massad, T., Medlyn, B. E., Messier, J., Moles, A. T., Müller, S. C., Nadrowski, K., Naeem, S., Niinemets, Ü., Nöllert, S., Nüske, A., Ogaya, R., Oleksyn, J., Onipchenko, V. G., Onoda, Y., Ordoñez, J., Overbeck, G., Ozinga, W. A., Patiño, S., Paula, S., Pausas, J. G., Peñuelas, J., Phillips, O. L., Pillar, V., Poorter, H., Poorter, L., Poschlod, P., Prinzing, A., Proulx, R., Rammig, A., Reinsch, S., Reu, B., Sack, L., Salgado-Negret, B., Sardans, J., Shiodera, S., Shipley, B., Siefert, A., Sosinski, E., Soussana, J. F., Swaine, E., Swenson, N., Thompson, K., Thornton, P., Waldrum, M., Weiher, E., White, M., White, S., Wright, S. J., Yguel, B., Zaehle, S., Zanne, A. E., and Wirth, C.: TRY - a global database of plant traits, *Global Change Biology*, 17, 2905–2935, <https://doi.org/10.1111/j.1365-2486.2011.02451.x>, <http://doi.wiley.com/10.1111/j.1365-2486.2011.02451.x>, <http://www.ncbi.nlm.nih.gov/pubmed/17388899>, <https://www.ncbi.nlm.nih.gov/pmc/articles/PMC3183702/>, <https://onlinelibrary.wiley.com/doi/10.1111/j.1469-8137.2007.02011.x>, <https://onlinelibrary.wiley.com/doi/10.1111/j.1365-2486.2011.02451.x>, 2011.
- Kattge, J., Bönisch, G., Díaz, S., Lavorel, S., Prentice, I. C., Leadley, P., Tautenhahn, S., Werner, G. D., Aakala, T., Abedi, M., Acosta, A. T., Adamidis, G. C., Adamson, K., Aiba, M., Albert, C. H., Alcántara, J. M., Alcázar C. C., Aleixo, I., Ali, H., Amiaud, B., Ammer, C., Amoroso, M. M., Anand, M., Anderson, C., Anten, N., Antos, J., Apgaua, D. M. G., Ashman, T. L., Asmara, D. H., Asner, G. P., Aspinwall, M., Atkin, O., Aubin, I., Bastrup-Spohr, L., Bahalkeh, K., Bahn, M., Baker, T., Baker, W. J., Bakker, J. P., Baldocchi, D., Baltzer, J., Banerjee, A., Baranger, A., Barlow, J., Barneche, D. R., Baruch, Z., Bastianelli, D., Battles, J., Bauerle, W., Bauters, M., Bazzato, E., Beckmann, M., Beeckman, H., Beierkuhnlein, C., Bekker, R., Belfry, G., Belluau, M., Belouï, M., Benavides, R., Benomar, L., Berdugo-Lattke, M. L., Berenguer, E., Bergamin, R., Bergmann, J., Bergmann Carlucci, M., Berner, L., Bernhardt-Römermann, M., Bigler, C., Bjorkman, A. D., Blackman, C., Blanco, C., Blonder, B., Blumenthal, D., Bocanegra-González, K. T., Boeckx, P., Bohlman, S., Böhning-Gaese, K., Boisvert-Marsh, L., Bond, W., Bond-Lamberty, B., Boom, A., Boonman, C. C., Bordin, K., Boughton, E. H., Boukili, V., Bowman, D. M., Bravo, S., Brendel, M. R., Broadley, M. R., Brown, K. A., Bruehlheide, H., Brunnich, F., Bruun, H. H., Bruy, D., Buchanan, S. W., Bucher, S. F., Buchmann, N., Buitenwerf, R., Bunker, D. E., Bürger, J., Burrascano, S., Burslem, D. F., Butterfield, B. J., Byun, C., Marques, M., Scalón, M. C., Caccianiga, M., Cadotte, M., Cailleret, M., Camac, J., Camarero, J. J., Campany, C., Campetella, G., Campos, J. A., Cano-Arboleda, L., Canullo, R., Carbognani, M., Carvalho, F., Casanoves, F., Castagneyrol, B., Catford, J. A., Cavender-Bares, J., Cerabolini, B. E., Cervellini, M., Chacón-Madrigal, E., Chapin, K., Chapin, F. S., Chelli, S., Chen, S. C., Chen, A., Cherubini, P., Chianucci, F., Choat, B., Chung, K. S., Chytrý, M., Ciccarelli, D., Coll, L., Collins, C. G., Conti, L., Coomes, D., Cornelissen, J. H.,

- Cornwell, W. K., Corona, P., Coyea, M., Craine, J., Craven, D., Cromsigt, J. P., Csecserits, A., Cufar, K., Cuntz, M., da Silva, A. C., Dahlin, K. M., Dainese, M., Dalke, I., Dalle Fratte, M., Dang-Le, A. T., Danihelka, J., Dannoura, M., Dawson, S., de Beer, A. J., De Frutos, A., De Long, J. R., Dechant, B., Delagrange, S., Delpierre, N., Derroire, G., Dias, A. S., Diaz-Toribio, M. H., Dimitrakopoulos, P. G., Dobrowolski, M., Doktor, D., Dřevojan, P., Dong, N., Dransfield, J., Dressler, S., Duarte, L., Ducouret, E., Dullinger, S., Durka, W., Duursma, R., Dymova, O., E-Vojtkó, A., Eckstein, R. L., Ejtehadi, H., Elser, J., Emilio, T., Engemann, K., Erfanian, M. B., Erfmeier, A., Esquivel-Muelbert, A., Esser, G., Estiarte, M., Domingues, T. F., Fagan, W. F., Fagúndez, J., Falster, D. S., Fan, Y., Fang, J., Farris, E., Fazlioglu, F., Feng, Y., Fernandez-Mendez, F., Ferrara, C., Ferreira, J., Fidelis, A., Finegan, B., Firn, J., Flowers, T. J., Flynn, D. F., Fontana, V., Forey, E., Forgiarini, C., François, L., Frangipani, M., Frank, D., Frenette-Dussault, C., Freschet, G. T., Fry, E. L., Fyllas, N. M., Mazzochini, G. G., Gachet, S., Gallagher, R., Ganade, G., Ganga, F., García-Palacios, P., Gargaglione, V., Garnier, E., Garrido, J. L., de Gasper, A. L., Gea-Izquierdo, G., Gibson, D., Gillison, A. N., Giroldo, A., Glasenhardt, M. C., Gleason, S., Gliesch, M., Goldberg, E., Göldel, B., Gonzalez-Akre, E., Gonzalez-Andujar, J. L., González-Melo, A., González-Robles, A., Graae, B. J., Granda, E., Graves, S., Green, W. A., Gregor, T., Gross, N., Guerin, G. R., Günther, A., Gutiérrez, A. G., Haddock, L., Haines, A., Hall, J., Hambuckers, A., Han, W., Harrison, S. P., Hattingh, W., Hawes, J. E., He, T., He, P., Heberling, J. M., Helm, A., Hempel, S., Hentschel, J., Héroult, B., Heresz, A. M., Herz, K., Heuertz, M., Hickler, T., Hietz, P., Higuchi, P., Hipp, A. L., Hirons, A., Hock, M., Hogan, J. A., Holl, K., Honnay, O., Hornstein, D., Hou, E., Hough-Snee, N., Hovstad, K. A., Ichie, T., Igic, B., Illa, E., Isaac, M., Ishihara, M., Ivanov, L., Ivanova, L., Iversen, C. M., Izquierdo, J., Jackson, R. B., Jackson, B., Jactel, H., Jagodzinski, A. M., Jandt, U., Jansen, S., Jenkins, T., Jentsch, A., Jespersen, J. R. P., Jiang, G. F., Johansen, J. L., Johnson, D., Jokela, E. J., Joly, C. A., Jordan, G. J., Joseph, G. S., Junaed, D., Junker, R. R., Justes, E., Kabzems, R., Kane, J., Kaplan, Z., Kattenborn, T., Kavelenova, L., Kearsley, E., Kempel, A., Kenzo, T., Kerkhoff, A., Khalil, M. I., Kinlock, N. L., Kissling, W. D., Kitajima, K., Kitzberger, T., Kjøller, R., Klein, T., Kleyer, M., Klimešová, J., Klipel, J., Kloeppe, B., Klotz, S., Knops, J. M., Kohyama, T., Koike, F., Kollmann, J., Komac, B., Komatsu, K., König, C., Kraft, N. J., Kramer, K., Kreft, H., Kühn, I., Kumarathunge, D., Kuppler, J., Kurokawa, H., Kurosawa, Y., Kuyah, S., Laclau, J. P., Lafleur, B., Lallai, E., Lamb, E., Lamprecht, A., Larkin, D. J., Laughlin, D., Le Bagousse-Pinguet, Y., le Maire, G., le Roux, P. C., le Roux, E., Lee, T., Lens, F., Lewis, S. L., Lhotsky, B., Li, Y., Li, X., Lichstein, J. W., Liebergesell, M., Lim, J. Y., Lin, Y. S., Linares, J. C., Liu, C., Liu, D., Liu, U., Livingstone, S., Llusià, J., Lohbeck, M., López-García, Á., Lopez-Gonzalez, G., Lososová, Z., Louault, F., Lukács, B. A., Lukeš, P., Luo, Y., Lussu, M., Ma, S., Maciel Rabelo Pereira, C., Mack, M., Maire, V., Mäkelä, A., Mäkinen, H., Malhado, A. C. M., Mallik, A., Manning, P., Manzoni, S., Marchetti, Z., Marchino, L., Marcilio-Silva, V., Marcon, E., Marignani, M., Markesteyn, L., Martin, A., Martínez-Garza, C., Martínez-Vilalta, J., Mašková, T., Mason, K., Mason, N., Massad, T. J., Masse, J., Mayrose, I., McCarthy, J., McCormack, M. L., McCulloh, K., McFadden, I. R., McGill, B. J., McPartland, M. Y., Medeiros, J. S., Medlyn, B., Meerts, P., Mehrabi, Z., Meir, P., Melo, F. P., Mencuccini, M., Meredieu, C., Messier, J., Mészáros, I., Metsaranta, J., Michaletz, S. T., Michelaki, C., Migalina, S., Milla, R., Miller, J. E., Minden, V., Ming, R., Mokany, K., Moles, A. T., Molnár, A., Molofsky, J., Molz, M., Montgomery, R. A., Monty, A., Moravcová, L., Moreno-Martínez, A., Moretti, M., Mori, A. S., Mori, S., Morris, D., Morrison, J., Mucina, L., Mueller, S., Muir, C. D., Müller, S. C., Munoz, F., Myers-Smith, I. H., Myster, R. W., Nagano, M., Naidu, S., Narayanan, A., Natesan, B., Negoita, L., Nelson, A. S., Neuschulz, E. L., Ni, J., Niedrist, G., Nieto, J., Niinemets, Ü., Nolan, R., Nottebrock, H., Nouvellon, Y., Novakovskiy, A., Nystruen, K. O., O'Grady, A., O'Hara, K., O'Reilly-Nugent, A., Oakley, S., Oberhuber, W., Ohtsuka, T., Oliveira, R., Öllerer, K., Olson, M. E., Onipchenko, V., Onoda, Y., Onstene, R. E., Ordonez, J. C., Osada, N., Ostonen, I., Ottaviani, G., Otto, S., Overbeck, G. E., Ozinga, W. A., Pahl, A. T., Paine, C. E., Pakeman, R. J., Papageorgiou, A. C., Parfionova, E., Pärtel, M., Patacca, M., Paula, S., Paule, J., Pauli, H., Pausas, J. G., Peco, B., Penuelas, J., Perea, A., Peri, P. L., Petisco-Souza, A. C., Petraglia, A., Petritan, A. M., Phillips, O. L., Pierce, S., Pillar, V. D., Pisek, J., Pomogaybin, A., Poorter, H., Portsmuth, A., Poschlod, P., Potvin, C., Pounds, D., Powell, A. S., Power, S. A., Prinzing, A., Puglielli, G., Pyšek, P., Raev, V., Rammig, A., Ransijn, J., Ray, C. A., Reich, P. B., Reichstein, M., Reid, D. E., Réjou-Méchain, M., de Dios, V. R., Ribeiro, S., Richardson, S., Riibak, K., Rillig, M. C., Riviera, F., Robert, E. M., Roberts, S., Robroek, B., Roddy, A., Rodrigues, A. V., Rogers, A., Rollinson, E., Rolo, V., Römermann, C., Ronzhina, D., Roscher, C., Rosell, J. A., Rosenfield, M. F., Rossi, C., Roy, D. B., Royer-Tardif, S., Rüger, N., Ruiz-Peinado, R., Rumpf, S. B., Rusch, G. M., Ryo, M., Sack, L., Saldaña, A., Salgado-Negret, B., Salguero-Gomez, R., Santa-Regina, I., Santacruz-García, A. C., Santos, J., Sardans, J., Schamp, B., Scherer-Lorenzen, M., Schleuning, M., Schmid, B., Schmidt, M., Schmitt, S., Schneider, J. V., Schowanek, S. D., Schrader, J., Schrodt, F., Schuldt, B., Schurr, F., Selaya Garvizu, G., Semchenko, M., Seymour, C., Sfair, J. C., Sharpe, J. M., Sheppard, C. S., Sheremetiev, S., Shiodera, S., Shipley, B., Shovon, T. A., Siebenkäs, A., Sierra, C., Silva, V., Silva, M., Sitzia, T., Sjöman, H., Slot, M., Smith, N. G., Sodhi, D., Soltis, P., Soltis, D., Somers, B., Sonnier, G., Sørensen, M. V., Sosinski, E. E., Soudzilovskaia, N. A., Souza, A. F., Spasojevic, M., Sperandii, M. G., Stan, A. B., Stegen, J., Steinbauer, K., Stephan, J. G., Sterck, F., Stojanovic, D. B., Strydom, T., Suarez, M. L., Svenning, J. C., Svitková, I., Svitok, M., Svoboda, M., Swaine, E., Swenson, N., Tabarelli, M., Takagi, K., Tappeiner, U., Tarifa, R., Tauugourdeau, S., Tavsanoglu, C., te Beest, M., Tedersoo, L., Thiffault, N., Thom, D., Thomas, E., Thompson, K., Thornton, P. E., Thuiller, W., Tichý, L., Tissue, D., Tjoelker, M. G., Tng, D. Y. P., Tobias, J., Török, P., Tarin, T., Torres-Ruiz, J. M., Tóthmérész, B., Treurnicht, M., Trivellone, V., Trolliet, F., Trotsiuk, V., Tsakalos, J. L., Tsiripidis, I., Tysklind, N., Umehara, T., Usoltsev, V., Vadéboncoeur, M., Vaezi, J., Valladares, F., Vamosi, J., van Bodegom, P. M., van Breugel, M., Van Cleemput, E., van de Weg, M., van der Merwe, S., van der Plas, F., van der Sande, M. T., van

- 215 Kleunen, M., Van Meerbeek, K., Vanderwel, M., Vanselow, K. A., Vårhammar, A., Varone, L., Vasquez Valderrama, M. Y., Vassilev, K.,  
Vellend, M., Veneklaas, E. J., Verbeeck, H., Verheyen, K., Vibrans, A., Vieira, I., Villacís, J., Violle, C., Vivek, P., Wagner, K., Waldram,  
M., Waldron, A., Walker, A. P., Waller, M., Walther, G., Wang, H., Wang, F., Wang, W., Watkins, H., Watkins, J., Weber, U., Weedon, J. T.,  
Wei, L., Weigelt, P., Weiher, E., Wells, A. W., Wellstein, C., Wenk, E., Westoby, M., Westwood, A., White, P. J., Whitten, M., Williams,  
M., Winkler, D. E., Winter, K., Womack, C., Wright, I. J., Wright, S. J., Wright, J., Pinho, B. X., Ximenes, F., Yamada, T., Yamaji, K.,  
Yanai, R., Yankov, N., Yguel, B., Zanini, K. J., Zanne, A. E., Zelený, D., Zhao, Y. P., Zheng, J., Zheng, J., Ziemińska, K., Zirbel, C. R.,  
Zizka, G., Zo-Bi, I. C., Zott, G., and Wirth, C.: TRY plant trait database – enhanced coverage and open access, *Global Change Biology*,  
26, 119–188, <https://doi.org/10.1111/gcb.14904>, 2020.
- 220 Krinner, G., Viovy, N., de Noblet-Ducoudré, N., Ogée, J., Polcher, J., Friedlingstein, P., Ciais, P., Sitch, S., and Prentice, I. C.: A dy-  
namic global vegetation model for studies of the coupled atmosphere-biosphere system, *Global Biogeochemical Cycles*, 19, 1–33,  
225 <https://doi.org/10.1029/2003GB002199>, <http://doi.wiley.com/10.1029/2003GB002199>, 2005.
- Largeron, C., Krinner, G., Ciais, P., and Brutel-Vuilmet, C.: Implementing northern peatlands in a global land surface model: Description  
225 and evaluation in the ORCHIDEE high-latitude version model (ORC-HL-PEAT), *Geoscientific Model Development*, 11, 3279–3297,  
<https://doi.org/10.5194/gmd-11-3279-2018>, 2018.
- Li, T., Raivonen, M., Alekseychik, P., Aurela, M., Lohila, A., Zheng, X., Zhang, Q., Wang, G., Mammarella, I., Rinne, J., Yu, L., Xie, B.,  
230 Vesala, T., and Zhang, W.: Importance of vegetation classes in modeling CH<sub>4</sub> emissions from boreal and subarctic wetlands in Finland,  
*Science of the Total Environment*, 572, 1111–1122, <https://doi.org/10.1016/j.scitotenv.2016.08.020>, <http://dx.doi.org/10.1016/j.scitotenv.2016.08.020>, 2016.
- Mi, Y., Van Huissteden, J., Parmentier, F. J. W., Gallagher, A., Budishchev, A., Berridge, C. T., and Dolman, A. J.: Improving a  
235 plot-scale methane emission model and its performance at a northeastern Siberian tundra site, *Biogeosciences*, 11, 3985–3999,  
<https://doi.org/10.5194/bg-11-3985-2014>, 2014.
- Müller, J. and Joos, F.: Global peatland area and carbon dynamics from the Last Glacial Maximum to the present – A process-based model in-  
vestigation, *Biogeosciences*, 17, 5285–5308, <https://doi.org/10.5194/bg-17-5285-2020>, <https://bg.copernicus.org/articles/17/5285/2020/>,  
2020.
- Ringeval, B., De Noblet-Ducoudré, N., Ciais, P., Bousquet, P., Prigent, C., Papa, F., and Rossow, W. B.: An attempt to quantify the impact of  
240 changes in wetland extent on methane emissions on the seasonal and interannual time scales, *Global Biogeochemical Cycles*, 24, 1–12,  
<https://doi.org/10.1029/2008GB003354>, 2010.
- Shi, X., Thornton, P. E., Ricciuto, D. M., Hanson, P. J., Mao, J., Sebestyen, S. D., Griffiths, N. A., and Bisht, G.: Representing northern  
245 peatland microtopography and hydrology within the Community Land Model, *Biogeosciences*, 12, 6463–6477, <https://doi.org/10.5194/bg-12-6463-2015>, [www.biogeosciences.net/12/6463/2015/](http://www.biogeosciences.net/12/6463/2015/), 2015.
- Sitch, S., Smith, B., Prentice, I. C., Arneth, A., Bondeau, A., Cramer, W., Kaplan, J. O., Levis, S., Lucht, W., Sykes, M. T., Thonicke, K.,  
250 and Venevsky, S.: Evaluation of ecosystem dynamics, plant geography and terrestrial carbon cycling in the LPJ dynamic global vegetation  
model, *Global Change Biology*, 9, 161–185, <https://doi.org/10.1046/j.1365-2486.2003.00569.x>, 2003.
- Smith, B., Prentice, I. C., and Sykes, M. T.: Representation of vegetation dynamics in the modelling of terrestrial ecosystems: comparing two  
255 contrasting approaches within European climate space, *Global Ecology and Biogeography*, 10, 621–637, <https://doi.org/10.1046/j.1466-822x.2001.t01-1-00256.x>, 2001.
- Stocker, B. D., Spahni, R., and Joos, F.: DYPTOP: A cost-efficient TOPMODEL implementation to simulate sub-grid spatio-temporal  
260 dynamics of global wetlands and peatlands, *Geoscientific Model Development*, 7, 3089–3110, <https://doi.org/10.5194/gmd-7-3089-2014>,  
2014.
- van Huissteden, J., van den Bos, R., and Marticorena Alvarez, I.: Modelling the effect of water-table management on CO<sub>2</sub> and CH<sub>4</sub> fluxes  
265 from peat soils, *Geologie en Mijnbouw/Netherlands Journal of Geosciences*, 85, 3–18, <https://doi.org/10.1017/S0016774600021399>,  
2006.
- van Huissteden, J., Petrescu, a. M. R., Hendriks, D. M. D., and Rebel, K. T.: Sensitivity analysis of a wetland methane emission model based  
270 on temperate and Arctic wetland sites, *Biogeosciences*, 6, 9083–9126, <https://doi.org/10.5194/bgd-6-9083-2009>, 2009.
- Walter, B. P. and Heimann, M.: A process-based, climate-sensitive model to derive methane emissions from natural wetlands:  
275 Application to five wetland sites, sensitivity to model parameters, and climate, *Global Biogeochemical Cycles*, 14, 745–765,  
<https://doi.org/10.1029/1999GB001204>, 2000a.
- Walter, B. P. and Heimann, M.: A process-based, climate-sensitive model to derive methane emissions from natural wetlands:  
280 Application to five wetland sites, sensitivity to model parameters, and climate, *Global Biogeochemical Cycles*, 14, 745–765,  
<https://doi.org/10.1029/1999GB001204>, 2000b.
- 285 Wania, R., Ross, L., and Prentice, I. C.: Integrating peatlands and permafrost into a dynamic global vegetation model: 1. Evaluation and  
sensitivity of physical land surface processes, *Global Biogeochemical Cycles*, 23, n/a–n/a, <https://doi.org/10.1029/2008GB003412>, <http://dx.doi.org/10.1029/2008GB003412>, 2009.

Wania, R., Ross, I., and Prentice, I. C.: Implementation and evaluation of a new methane model within a dynamic global vegetation model: LPJ-WHyMe v1.3.1, *Geoscientific Model Development*, 3, 565–584, <https://doi.org/10.5194/gmd-3-565-2010>, 2010.

270 Wu, J., Roulet, N. T., Moore, T. R., Lafleur, P., and Humphreys, E.: Dealing with microtopography of an ombrotrophic bog for simulating ecosystem-level CO<sub>2</sub> exchanges, *Ecological Modelling*, 222, 1038–1047, <https://doi.org/10.1016/j.ecolmodel.2010.07.015>, <http://dx.doi.org/10.1016/j.ecolmodel.2010.07.015>, 2011.

275 Wu, Y., Verseghy, D. L., and Melton, J. R.: Integrating peatlands into the coupled Canadian Land Surface Scheme (CLASS) v3.6 and the Canadian Terrestrial Ecosystem Model (CTEM) v2.0, *Geoscientific Model Development*, 9, 2639–2663, <https://doi.org/10.5194/gmd-9-2639-2016>, <https://gmd.copernicus.org/articles/9/2639/2016/>, 2016.

Yurova, A., Wolf, A., Sagerfors, J., and Nilsson, M.: Variations in net ecosystem exchange of carbon dioxide in a boreal mire: Modeling mechanisms linked to water table position, *Journal of Geophysical Research: Biogeosciences*, 112, G02 025, <https://doi.org/10.1029/2006JG000342>, <http://doi.wiley.com/10.1029/2006JG000342>, 2007.